Flow visualization and study of CHF enhancement in pool boiling with Al2O3 - Water nano-fluids

Article *in* Thermal Science · January 2011

DOI: 10.2298/TSCI100511095H

CITATIONS
17

READS
81

3 authors, including:

Ramakrishna N Hegde
Srinivas Group of Colleges
26 PUBLICATIONS **116** CITATIONS

SEE PROFILE

FLOW VISUALIZATION AND STUDY OF CRITICAL HEAT FLUX ENHANCEMENT IN POOL BOILING WITH Al_2O_3-WATER NANOFLUIDS

by

Ramakrishna N. HEGDE [a*], ***Shrikantha S. RAO*** [b], ***and Ranapratap REDDY*** [c]

[a] National Institute of Technology, Surathkal, and Faculty, M. S. Ramaiah Institute of Technology, Bangalore, India
[b] Department of Mechanical Engineering, National Institute of Technology, Surathkal, India
[c] Reva Institute of Technology, Yelahanka, Bangalore, India

Original scientific paper
DOI: 10.2298/TSCI100511095H

Pool boiling heat transfer characteristics of Al_2O_3-water nanofluids is studied experimentally using a NiCr test wire of 36 standard wire guage diameter. The experimental work mainly concentrated on (1) change of critical heat flux with different volume concentrations of nanofluid and (2) flow visualization of pool boiling using a fixed concentration of nanofluid at different heat flux values. The experimental work revealed an increase in critical heat flux value of around 48% and flow visualization helped in studying the pool boiling behaviour of nanofluid. Out of the various reasons which could affect the critical heat flux enhancement, surface roughness plays a major role in pool boiling heat transfer.

Key words: *nanofluid, critical heat flux, flow visualization, surface roughness*

Introduction

Heat transfer can be most efficient if heat can be removed from a hot surface in the form of heat of vaporization and sensible heat. The benefit of heat transfer can be taken when a liquid coolant undergoes phase change and thereby absorbing heat from a solid surface. Heat transfer with phase change is not an uncommon phenomenon. Industrial systems like boilers, condensers, cooling systems, *etc.* utilize phase change to the fullest extent. An extensive literature survey reveals that comparatively less research work has been reported about phase change of a fluid or boiling phenomenon and in particular heat transfer considering the economical efficiency of the systems. Critical heat flux (CHF) is the condition where the vapor generated by nucleate boiling becomes so large that it prevents the liquid from reaching and re-wetting the surface. Pool boiling CHF is the point where nucleate boiling goes through a flow regime transition to film boiling with a continuous vapor film separating the heater and the liquid.

So far the research work revolved around experimental and theoretical studies concerning CHF under forced convection boiling conditions leading to many models and methods.

* Corresponding author; e-mail: rkhegderk@gmail.com

Due to contradictory claims by researchers and economic view point CHF continues to be studied still by the researchers. Some of the notable contributions in this area are discussed in the following paragraph.

In a pool boiling experiment at the pressure of 20.89 kPa You *et al.* [1] demonstrated that the CHF of Al_2O_3-water increased about 200% compared with pure water without any change in the nucleate boiling heat transfer coefficient.

Das *et al.* [2] conducted an investigation on the pool boiling of Al_2O_3-water nanoparticles-suspension on a horizontal tubular heater of 20 mm diameter. They observed deterioration of the boiling heat transfer of nanoparticle compared to that of pure water.

Vassallo *et al.* [3] carried out a pool experiment of silica-water nanoparticles-suspensions on a horizontal NiCr wire at atmospheric pressure without using any surfactants. They reported CHF enhancement to the extent of 30% for horizontal and 13% for vertical flat surface in the pool.

Bang *et al.* [4] investigated on the pool boiling of Al_2O_3-water nanoparticles-suspensions on a plain plate at atmospheric pressure without using any surfactant. The CHF of the nanofluid increased 32%.

Wen [5] investigated the role of structural disjoining pressure arising from the confinement of nanoparticles in a meniscus in CHF enhancement. He claimed that structural disjoining pressure can significantly increase the wettability of the fluids and inhibit dry patch development.

Kwark *et al.* [6] studied pool boiling behavior of low concentration nanofluids (≤1 g/l) experimentally over a flat heater at 1 atm. They guessed boiling of nanoparticles produce a thin film on the heater surface is responsible for increase in CHF.

CHF prediction was first addressed by Kutateladze [7]. He proposed the relation (1) to study saturated pool boiling:

$$K = \frac{q}{\rho_g h_{fg} \sqrt[4]{\dfrac{\sigma(\rho_f - \rho_g)g_e}{\rho_g^2}}} \tag{1}$$

where K is a constant equal to 0.16 for pool boiling from a large horizontal pool surface.

In the later stage Zuber [8] introduced the following relation to determine the CHF:

$$\frac{q_c}{h_{fg}\rho_v^{0.5}\sqrt[4]{\sigma g(\rho_l - \rho_v)}} = 0.131 \tag{2}$$

Preparation and characterization of nanofluid

Preparation and characterization of nanofluids

Nanofluid in different volume concentrations ranging from 0.01% to 0.1% were prepared by the two-step method, dispersing dry nanoparticles into the base liquid (distilled water) without any additives. For proper dispersion of nanoparticles in to the base fluid a high speed homogenizer was used and the liquid was stirred for 3 hours just before pool boiling experiments. The nanofluid properties are calculated using the established relations [9-14]. Further, TEM image taken showed (fig. 1) that nanoparticles were spherical in shape and not agglomerated and the size distribution of nanoparticles ranged between 10 to 80 nm.

CHF experiments with NiCr wire

Figure 2 shows the experimental set-up used in this work. The main test pool consists of a 250 mm diameter, 150 mm high pyrex glass vessel and a 30 mm thick bakelite cover. The simple geometry and glass material of the test chamber ensures clean conditions. A horizontally suspended smooth NiCr wire (test wire) of 0.19 mm diameter was used as a boiling surface. Both ends of the NiCr wire heater were tightly secured to the clamps of the tungsten electrodes. The heat input to the test wire was measured by a digital Watt meter incorporated with "critical heat input sensor".

The working fluid can be pre-heated using a 1 kW heating coil wound around a metallic strip of tungsten material. The pool temperature is measured with a RTD thermocouple of K-type. The liquid temperature is measured using another thermocouple inserted through the top of the bakelite cover plate (10 mm diameter hole). The cover plate can be secured firmly on to the glass vessel containing nanofluid. The hole on the cover ensures atmospheric conditions inside the vessel. The loss due to evaporation and liquid leakage (1.33%) was compensated by adding the makeup fluid before the next run.

All pool boiling experiments were conducted after the bulk temperature of the working fluid was stabilized at the saturated temperature (100 °C).

Figure 1. TEM photograph of Al_2O_3 nanoparticles

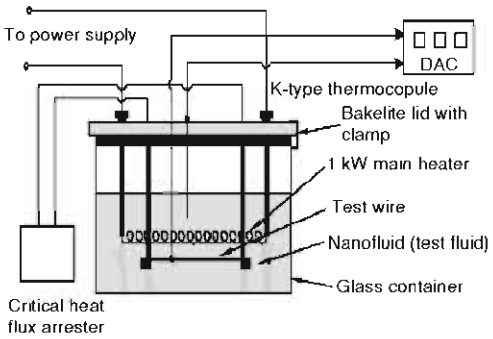

Figure 2. Experimental set-up

The experiment was conducted by increasing the electric power supplied to the wire heater (test wire). The electric power/heat input was increased in small steps using the variac until critical value is reached at which point, the heater was instantaneously broken due to increased resistance. The CHF was calculated using data obtained just before the steep increase of heater resistance. The peak value of wattage thus recorded is used to compute the critical heat flux as:

$$q = \frac{W}{A} \tag{3}$$

Uncertainty analysis [15] considering the main sources of uncertainty, viz. the applied wattage, contact resistance between the wire heater and electrodes which are connected with only mechanical clamps, length and diameter of the NiCr wire heater showed that the uncertainties of the applied voltage and the length and diameter of wire heater are less than 3.96% and 0.7%, respectively. From the above analysis, the maximum uncertainty for pool boiling CHF was estimated to be 4.96%.

Results and discussions

Figure 3 shows the measured CHF values of Al_2O_3 nanofluid at different volume concentrations.

Significant CHF enhancement is observed for all nanofluids, up to 48% with Al_2O_3 nanofluids as shown in fig. 4.

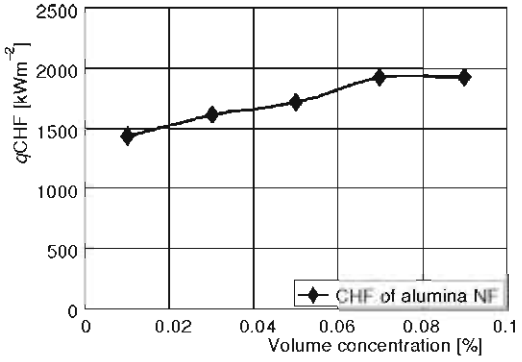

Figure 3. Variation of CHF with different volume concentrations of Al_2O_3 nanofluid

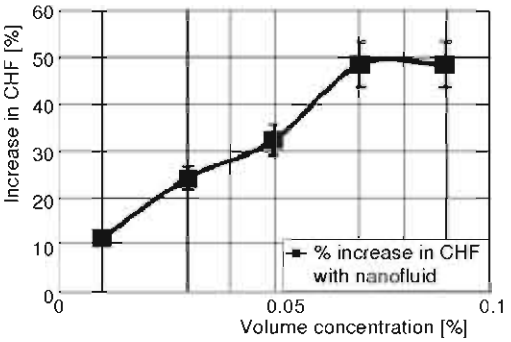

Figure 4. Percentage increase in CHF with Al_2O_3 compared pure water

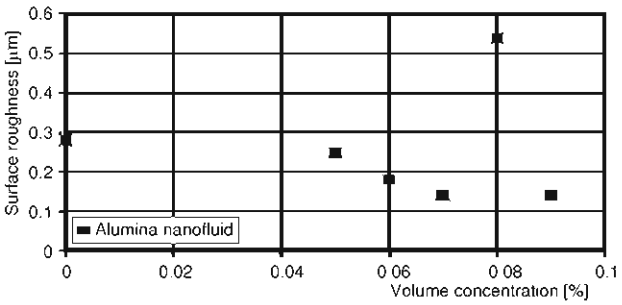

Figure 5. Variation in surface roughness with different volume concentrations of Al_2O_3 nanofluid

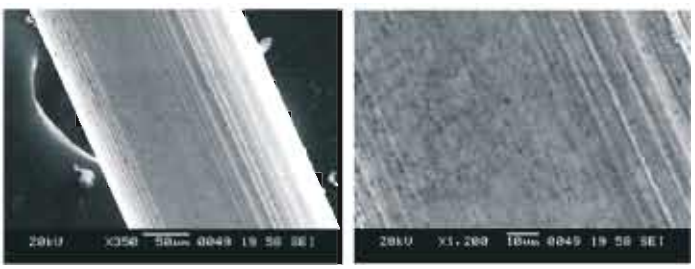

Figure 6. SEM image of bare heater surface

The nanofluids have higher CHF when compared to water. Surface roughness measurement of the test wire indicated the accumulation of nanoparticles. This can be attributed to the porous layer formed due to boiling induced precipitation of nanoparticles which was confirmed by surface testing. Figure 5 shows the variation of surface roughness with different volume concentrations of alumina nanofluid.

The presence of a porous layer on the surface definitely plays major role on boiling heat transfer through changes in roughness and wettability.The detailed study of the SEM image clearly showed deposition of the nanoparticles on the wire surface. Figure 6 shows the SEM image of the bare heater surface and subsequent fig-

ures 7 (a), (b), (c), and (d) show the heater surface after reaching the CHF at volume concentrations of 0.05%, 0.07%, 0.08%, and 0.1%, respectively. It can be observed that the deposition is more pronounced on the heater surface with 0.1% of Al_2O_3 nanofluid while at 0.08% it closely resembles to the bare heater surface.

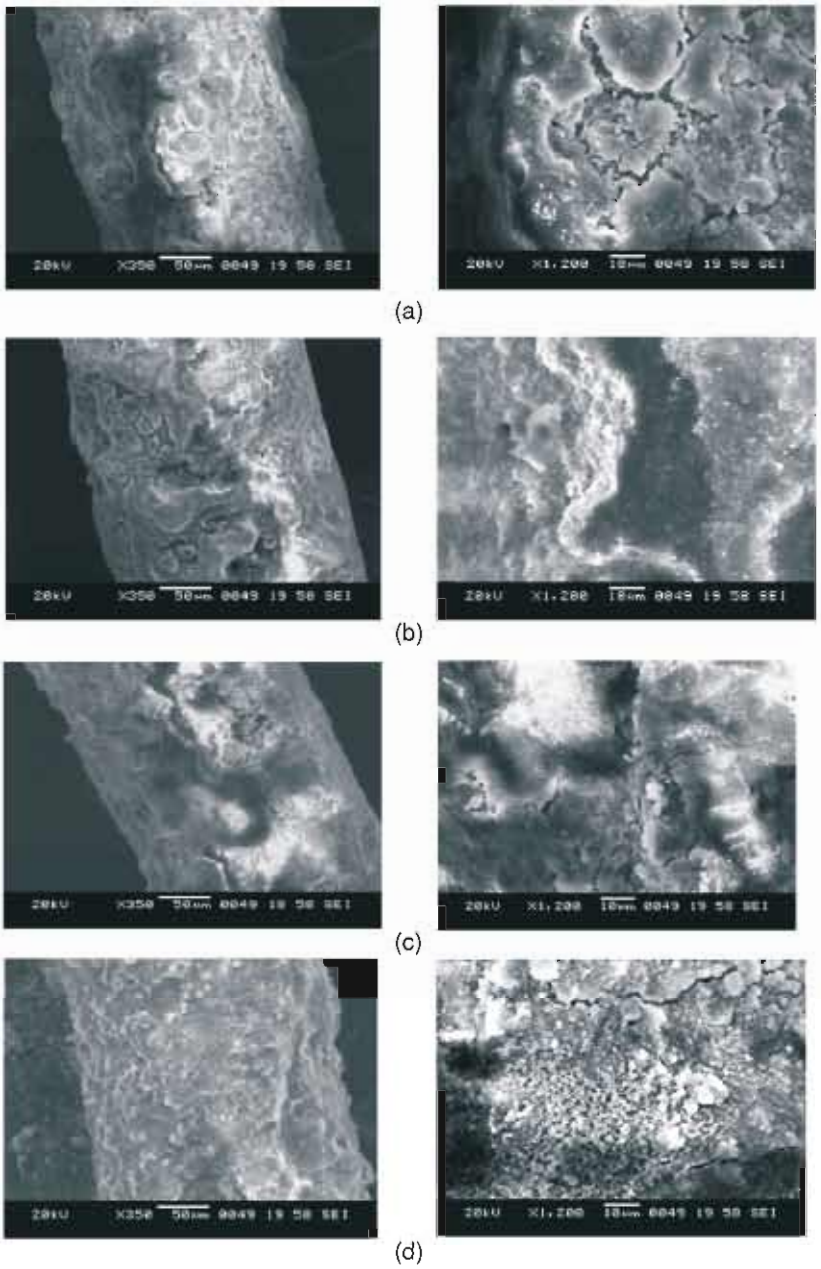

Figure 7. SEM image of heater surface with (a) 0.05%, (b) 0.07%, (c) 0.08%, and (d) 0.1% by volume of Al_2O_3 nanofluid

Flow visualization

The boiling phenomenon was observed using Nikon high speed digital camera with a shutter speed of 1/8000 s. The bubble generation, bubble growth, and subsequent bubble departure from the surface was clearly observed at different heat inputs in the increasing order till burnout point was reached. Since it is not possible to visualize the bubble growth phenomenon at higher concentration of alumina nanoparticles, a low concentration of 1 g/l of distilled water was used. The bubble growth behavior seems to be more or less similar to pure water [16]. Massive vapour clot was observed near the CHF value due to coalescence of bubbles. This is a very significant development as these vapors will have dry patches which ultimately affect the heat transfer.

Referring fig. 8, due to enough wall superheat, vapour nucleation starts to begin at the heating surface. In the initial stages few individual sites develop at lower heat flux. The site density and the bubble size increase as the heat flux is increased as shown in figs. 9 and 10. The size and shape of vapour bubbles departing from the heated surface depend on the way they are formed. The phenomenon of bubble growth can be attributed to two forces.

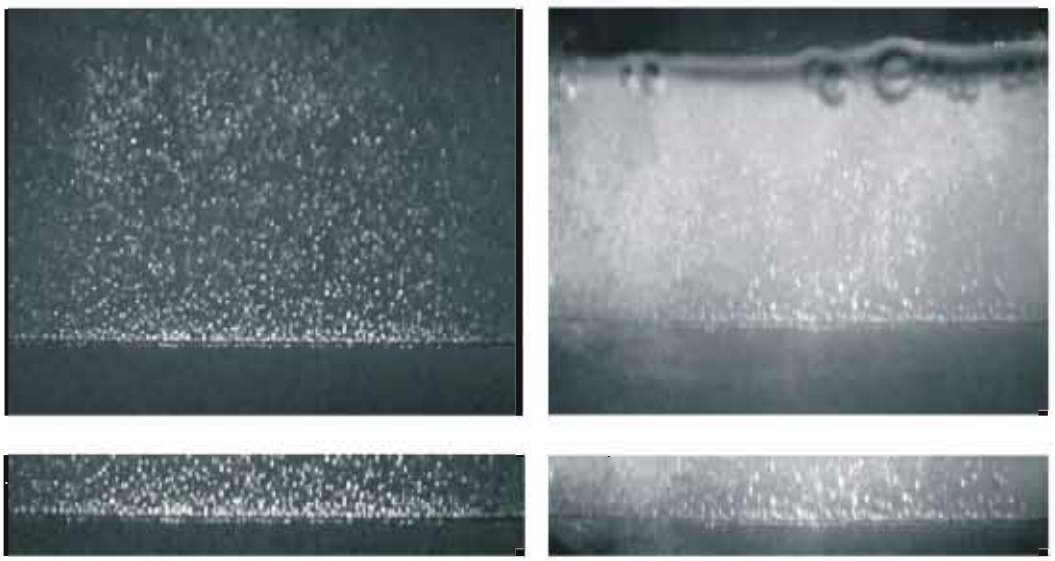

(a) 419 kW/m^2 (b) 670 kW/m^2

Figure 8. (a) Bubbles of small diameter appear on the surface of the test wire exposed to 419 kW/m^2 heat input continuously. Bubbles generate and collapse; (b) Bubbles grow in size when the heat flux was increased to 670 kW/m^2 and leave the surface

(1) Detaching force: the main forces responsible for this are buoyancy and hydrodynamic drag forces, and
(2) Attaching force: the main force that prevents bubble detachment is liquid inertia force due to the displacement of liquid during bubble growth.

The growth velocity of the bubble and the inertial force are a strong function of liquid superheat and is inversely proportional to the size of the active cavity. According to

Hatton *et al.* [17], for small cavity sizes of <10 μm (for water at atmospheric pressure) the bubble size is dictated mainly by a balance between buoyancy and inertia forces. For larger cavities bubble size departure is due the balance between buoyancy and surface tension forces. This is because as the growth rate is faster here resulting in smaller dynamic forces.

Fritz [18] suggested the following equation to determine the bubble departure diameter given by:

$$D_d = 0.204\theta\sqrt{\frac{\sigma}{g(\rho_1 - \rho_v)}} \tag{4}$$

where, the contact angle for nanofluid can be taken as 22-30°.

By knowing the bubble diameter D_d the nucleation site density, n can be calculated using the relation:

$$n = \frac{1}{D_d^2} \tag{5}$$

Under the influence of dominant surface tension forces the departing bubbles tend to be spherical and, under the dominant inertial forces they tend to be hemispherical. When both forces are significant the bubbles become oblate.

Since individual nucleation sites emit bubble with constant frequency given by the relation:

$$fD_d = 0.59\sqrt{\frac{\sigma g(\rho_1 - \rho_v)}{\rho_1^2}} \tag{6}$$

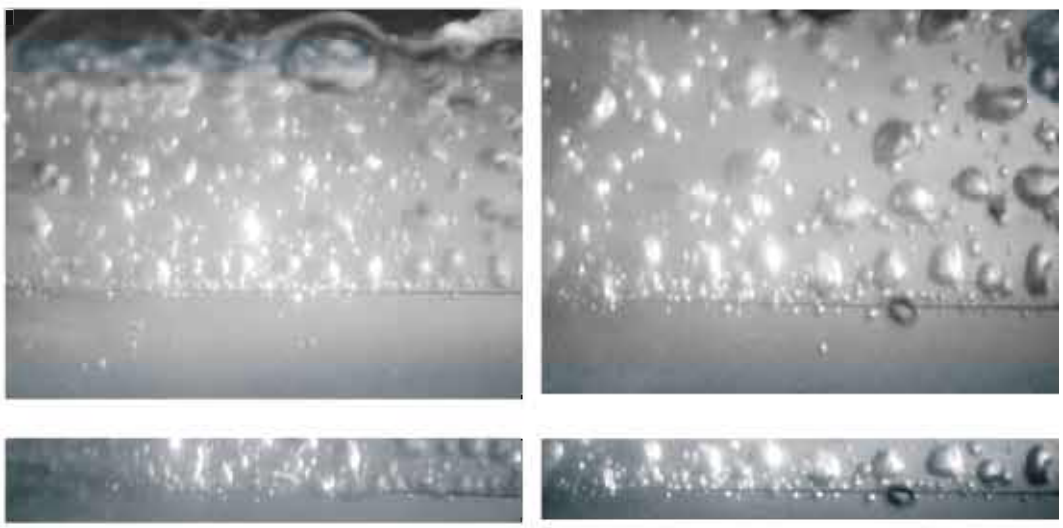

Figure 9. (a) Bubbles coalesce and grow bigger in size and rapidly appear on the surface of the test wire exposed to 922 kW/m^2 and detach from the surface; (b) Large coalesced bubbles can be seen when the heat flux was increased to 1139 kW/m^2

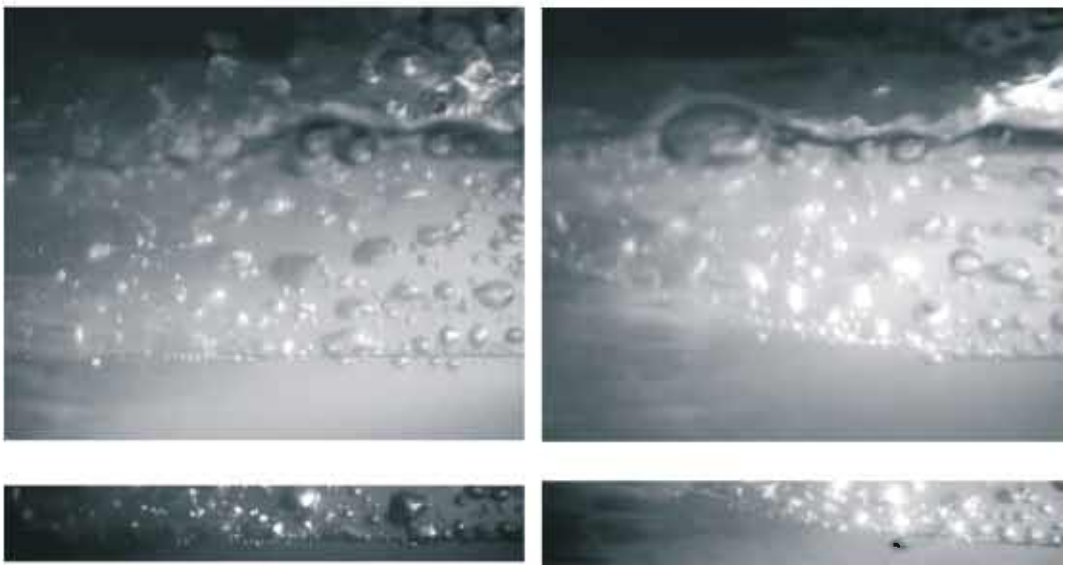

(a) 1307 kW/m^2 (b) At CHF

Figure 10. (a) Massive vapour bubbles appear on the surface of the test wire exposed to 1307 kW/m^2 heat input continuously and leave the surface. Bubble density is also higher; (b) Bubbles grow in size when the heat flux was increased to CHF value, of 1408 kW/m^2

Conclusions

Pool boiling CHF characteristics in Al_2O_3 nanofluids were investigated with different volume concentrations ranging from 0.01% to 0.1%, and the effect of nanoparticles in pool boiling CHF of Al_2O_3 nanofluids for each concentration was studied experimentally. During the experimentation, the pool boiling CHF of Al_2O_3 nanofluids on a bare heater of NiCr wire was enhanced to ~48% compared to that of pure water.

This study clearly showed that CHF enhancement of nanofluids was due to the nanoparticle surface coating formed on the heater surface during pool boiling. Surface roughness measurement and subsequent SEM images of the heater surface substantiated this. Formation of porous layer with micro cavities and subsequent deposition of nanoparticles resulted in enhancement in CHF.

Boiling phenomenon visualized at different heat input conditions clearly showed formation of massive vapour bubbles forming hot/dry spots. These dry spots develop at certain nucleation sites and on bubble departure if they do not rewet the surface; temperature of the test wire sharply increases resulting in burn out.

Additional work is needed to study the characterization of layer growth to understand the whole mechanism.

Nomenclature

A – surface area, [m^2]
D_d – bubble departure diameter, [m]
f – buble frequency, [s^{-1}]
g – gravitational acceleration, [ms^{-2}]
h_{fg} – latent heat of vaporization, [Jkg^{-1}]

k – thermal conductivity, [$Wm^{-1}K^{-1}$]
n – site density, [m^{-2}]
q – heat flux, [$Wm^{-2}K^{-1}$]
W – watt, [W]

Greek symbols

θ – contact angle, [deg.]
ρ – density, [kgm^{-3}]
σ – surface tension, [Nm^{-1}]

Subscripts

c – critical
l – liquid
v – vapour

References

[1] You, S. M., Kim, J., Kim, K. H., Effect of Nanoparticles on Critical Heat Flux of Water in Pool Boiling Heat Transfer, *Applied Physics Letters., 83* (2003), 16, pp. 3374-3376
[2] Das, S., Putra, N., Roetzel, W., Pool Boiling Characteristics of Nanofluids, *International Journal Heat and Mass Transfer, 46* (2003), 5, pp. 851-862
[3] Vassallo, P., Kumar, R., Amico, S. D., Pool Boiling Heat Transfer Experiments in Silica-Water Nanofluids, *International Journal of Heat and Mass Transfer, 47* (2004), 2, 407-411
[4] Bang, I. C., Chang, S. H., Boiling Heat Transfer Performance and Phenomena of Al_2O_3-Water Nanofluids from a Plain Surface in a Pool, *International Journal of Heat and Mass Transfer, 48* (2005), 12, pp. 2407-2419
[5] Wen, D., Mechanisms of Thermal Nanofluids on Enhanced Critical Heat Flux (CHF), *International Journal of Heat and Mass Transfer, 51* (2008), 19-20, pp. 4958-4965
[6] Kwark, S. M., *et al.*, Pool Boiling Characteristics of Low Concentration Nanofluids, *International Journal of Heat and Mass Transfer, 53* (2010), 5-6, 972-981
[7] Kutateladze, S. S., A Hydrodynamic Theory of Changes in the Boiling Process under Free Convection Conditions, Izv. Akad. Nauk, USSR, Otd. Tekh. Nauk, *4* (1951), pp. 529-935
[8] Zuber, N., Hydrodynamic Aspects of Boiling Heat Transfer, AEC report, AECU 4439, Los Angeles, Cal., USA, 1959
[9] Murshed, S. M. S., Leong, K. C., Yang, C., Enhanced Thermal Conductivity of TiO_2-Water Based Nanofluids, *Int. J. Thermal Sci., 44* (2005), 4, pp. 367-373
[10] Eastman, J. A., et al., Anomalously Increased Effective Thermal Conductivities of Ethylene Glycol-Based Nanofluids Containing Copper Nanoparticles, *Appl. Phys. Lett., 78* (2001), pp. 718-720
[11] Das, S. K., *et al.*, Temperature Dependence of Thermal Conductivity Enhancement for Nanofluids, *J. Heat Transfer, Trans. ASME, 125* (2003), 4, pp. 567-574
[12] Lee, S., *et al.*, Measuring Thermal Conductivity of Fluids Containing Oxide Nanoparticles, *ASME J. Heat Transfer, 121* (1999), 2, pp. 280-289
[13] Das, K., Putra, N., Roetzel, W., Pool Boiling Characteristics of Nanofluids, *Int. J. Heat Mass Transfer, 46* (2003), 5, pp. 851-862
[14] Brinkman, H. C., The Viscosity of Concentrated Suspensions and Solutions, *J. Chem. Phys., 20* (1952), 4, pp. 571-581
[15] Holman, J. P., Experimental Methods for Engineers, 7th ed., Chap. 3, McGraw-Hill, New York, USA, 2007
[16] Kim, S. J., *et al.*, Study of Pool Boiling and Critical Heat Flux Enhancement in Nanofluids, *Bulletin of the Polish Academy of Sciences, Technical Sciences, 55* (2007), 20, pp. 211-216
[17] Haton, A. P., McHall, J. P., Photographic Study of Boiling Prepared Surfaces, 3rd International Conference Heat Transfer Conference, Chicago, Ill., USA, 1966
[18] Fritz, W., Calculation of the Maximum Volume of Vapour Bubbles, *Physik Zeitschr., 36* (1935), pp. 379-384

Paper submitted: May 11, 2010
Paper revised: July 24, 2010
Paper accepted: August 31, 2011